High-Fidelity Large-Eddy Simulation of a Pulsed Jet Actuator

Özgür Yalc, Xavier Gloerfelt, Georges Saliba, Ahmad Batikh, Lucien Baldas

High-Fidelity Large-Eddy Simulation of a Pulsed Jet Actuator

Özgür Yalçın, Xavier Gloerfelt, Georges Saliba, Ahmad Batikh, and Lucien Baldas

1 Introduction

Pulsed jet actuators (PJAs) are a type of fluidic oscillators that can be served as an active flow control device on lifting bodies. PJAs are able to provide an unsteady periodic blowing in a wide frequency range, which adds momentum to the boundary layer to prevent separation, and thereby enhancing the aerodynamic performances [2]. This kind of fluidic oscillator has no moving parts and induces the oscillation using only its internal unsteady flow dynamics, which makes it attractive for applications given its robust design and installation [9].

The geometry of the PJA examined in this study is given in Figure 1. A jet through a nozzle that is supplied by a pressurized flow in a reservoir attaches on the side wall of one of the branches due to the Coanda effect [5]. While the flow partially exits from the actuator outlet located on the same side, the bi-stable attached flow starts to fill the feedback loop with a compression wave. When this wave reaches the control nozzle, it triggers a detachment of the attached jet, which is followed by a recirculation bubble growing between the side wall and the jet. Meanwhile, an expansion wave reflected from the control nozzle travels back to the branch exit. This back-and-forth traveling of the pressure wave inside the loop causes pressure differences between the two branch exits as well as the two control nozzles [10]. The combined effect of these pressure differences and the recircula-

Özgür Yalçın · Xavier Gloerfelt
Laboratoire DynFluid, Arts et Métiers Institute of Technology, Paris, France, e-mail: {ozgur.yalcin,xavier.gloerfelt}@ensam.eu

Georges Saliba · Lucien Baldas
Institut Clément Ader (ICA), Univ. Toulouse, CNRS, INSA, ISAE-SUPAERO, Mines Albi, UPS, Toulouse, France, e-mail: {saliba,baldas}@insa-toulouse.fr

Ahmad Batikh
Institut Clément Ader (ICA), Univ. Toulouse, CNRS, INSA, ISAE-SUPAERO, Mines Albi, UPS, Icam Toulouse, Toulouse, France, e-mail: ahmad.batikh@icam.fr

tion zone growth make the jet switch to the other side, and the same procedure is repeated. The switching of the jet provides an oscillatory blowing at the outlets.

The oscillation period, which is one of the critical design parameters in active flow control, is simply a combination of the travel time of the pressure waves inside the feedback loops and the switching time of the main jet. As the feedback loop length increases, the switching time becomes negligible. For this scenario, some simple algebraic formulas suggested in literature can provide reasonable prediction of the oscillation frequencies. However, the switching time still remains a mystery. There have been very few studies focused on understanding the switching period, which are mainly restricted to subsonic nozzle jets [7]. Besides, most of the numerical studies on this topic are based on unsteady Reynolds-Averaged Navier-Stokes (URANS) simulations. Although URANS approaches could predict the frequency of the oscillations having negligible switching time, they failed to predict the magnitude and profile of the exit velocity [10, 1], which is another critical design parameter. In order to obtain internal and external flow fields accurately, and to understand the unsteady and highly compressible flow dynamics of the switching phenomenon, a high-fidelity numerical analysis is required [6]. For this purpose, a high-order Large-Eddy Simulation (LES) inside of the PJA studied in [8] has been performed and analyzed in the present study. This PJA, also shown in Figure 1, has relatively short feedback loops, yielding a non negligible switching time. It thus constitutes a good test case to investigate the mechanisms behind the switching time.

This paper includes the solver description, the computational setup, and the numerical results with discussions. The result section is mainly focused on the comparisons with measurements and URANS results, which are described in [8].

2 Flow Solver and Computational Setup

The numerical simulation is performed using a research code, called MUSICAA (MUltiscale Solver In Computational Aeroacoustics and Aerodynamics). The 3D filtered compressible Navier-Stokes equations are solved by a wall-resolved LES (WRLES) strategy that models the subgrid motions numerically with a Regularization Term approach, i.e. without using an explicit subgrid scale model. The inviscid fluxes are discretized by means of 10^{th}-order standard centred differences whereas 4^{th}-order is used for viscous fluxes. In order to introduce a minimal amount of numerical dissipation while ensuring computational robustness for compressible flow simulations, the centered scheme is supplemented by a high-order nonlinear filtering term, combining 2^{nd}- and 10^{th}-order derivatives approximated by standard central differences. The activation of the low-order term rests on a modified Jameson's pressure-based shock sensor. A four-stage Runge-Kutta algorithm is used for time integration and a 4^{th}-order implicit residual smoothing method (IRS4) is implemented to enlarge the stability and allow the use of larger timesteps. The curvilinear grid is taken into account by a coordinate transformation. More details can be found in [4].

The computational domain covers both the internal and external fields of the PJA, from the inlet reservoir to the farfield. Figure 1 shows the multiblock domain with structured grids. A subsonic inlet boundary condition based on Riemann invariants is enforced at the inlet by specifying the ratios of the inlet total pressure to the freestream static one ($p_{t,in}/p_{fs}$). At the farfield boundaries, non-reflective boundary conditions based on asymptotic solutions of linearized Euler equations are applied. All walls are treated by no-slip conditions. The 2D domain given in Figure 1 has the same internal geometry as the experimented PJA, where the nozzle width is 0.2 mm. The domain is extruded uniformly along the third direction where periodicity is enforced. The reason is that in the experiment, the depth-to-width ratio is 35, which is assumed to be large enough to neglect the depthwise wall effects. The depth of the computational domain is chosen as 2.5 times of the nozzle exit width, considering the jet size which is limited by the distance between the nozzle exit and the splitter edge as well as the branch inlet widths. The mesh generation for each block is started by taking the non dimensional first cell height as 1 wall unit. The maximum streamwise grid spacing is 30 wall units, whereas the spanwise one is 15. In the whole domain, the grid stretching ratios are no more than 1.05. In total, the grid consists of approximately 1 million nodes in 2D, and has 30 nodes in the third direction.

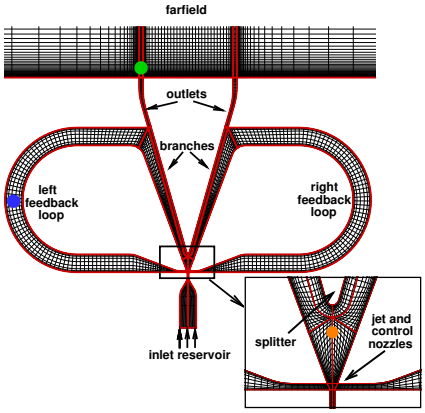

Fig. 1 Multiblock structured grid of the PJA. Every four cells are shown. The subframe zooms the switching area.

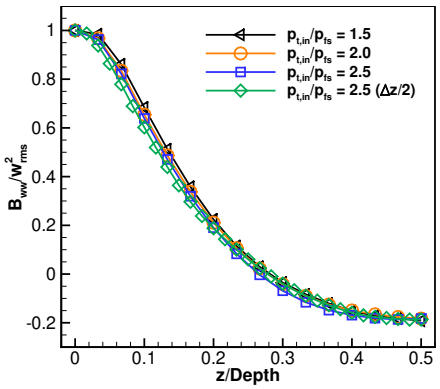

Fig. 2 Nondimensional two-point spanwise correlation at the center of the jet switching region.

3 Results

The simulations are performed for three different $p_{t,in}/p_{fs}$ values: $1.5, 2.0$, and 2.5. For each simulation, approximately 1000 CPU processors are used, each of which

has a single domain with $30 \times 30 \times 30$ grid nodes. The time steps are 5.0×10^{-9} s, 3.5×10^{-9} s, and 1.5×10^{-9} s for the lowest to the highest pressure ratios, respectively. Note that thanks to the IRS4 method, these time steps are around 8 times those limited by the explicit time scheme.

The simulations are carried out for more than 15 oscillation periods after the initial transients have left the computational domain. Before collecting data, a grid dependency study has been done to make sure that the grid resolution is sufficient. In this respect, two-point correlations are investigated, as proposed in [3]. Figure 2 shows the nondimensional two-point spanwise correlation variations, B_{ww}/w^2_{rms}, which are computed using time signals of third velocity component, w, for all pressure ratios at a point located at the center of the jet switching region (orange point in Figure 1). The figure also includes the results for the highest pressure ratio when the spanwise grid spacing (Δz) is divided by two. It is observed that the correlations go to zero within 10 grid points when Δz is used. It means the largest eddy scale is discretized by 10 nodes, which is sufficient [3]. Besides, using $\Delta z/2$ does not change the trend. Hence, the present grid spacing is kept for the rest of the study.

The oscillation frequency variations as a function of the pressure ratios are compared in Figure 3 with the measured data as well as URANS simulations based on two different modeling approaches, k-γ SST and k-ω SST with $\gamma - Re_\theta$ transition model. It is worth noting that the jet is choked beyond $p_{t,in}/p_{fs}$ of 1.7 such that the case with $p_{t,in}/p_{fs}$ of 1.5 is the only one where the jet is subsonic at the throat. It is observed from the measurements that after the jet is choked, the oscillation frequency decreases as the pressure ratio increases up to a certain point, and then remains almost constant. In the region of interest, the frequencies of the current study, indicated as WRLES in Figure 3, are in much more better agreement with the measurements than the URANS ones, even if WRLES predictions show a slight overestimation.

Instantaneous Mach contours are presented in Figure 4 for the case with $p_{t,in}/p_{fs}$ of 2.0, at an instant corresponding to the jet switching from left to right. The unsteadiness of the switching process, which includes the evolution of the recirculation and separation bubbles, can be observed by looking at the streamlines in the right subframe of the figure. Moreover, the flow is choked at the nozzle throat at this pressure ratio, and during the switching shocklets appear in the vicinity of the impingement onto the splitter. In addition, this region involves not only the most energetic turbulent structures but also the smallest ones in the domain. This is why the grid dependency study was conducted at the center of this region. On the other hand, this is an indication of the necessity of proper eddy resolution during the jet switching, explaining the failure of URANS when switching time is non negligible. One can also observe from the left subframe of Figure 4 that the jet is unsteady throughout the branch after it is detached from the corresponding side wall.

Figure 5 shows a comparison of the pressure norms (Z-score) for one oscillation period at the location of the left loop center (blue point in Figure 1). The results are given for the case with $p_{t,in}/p_{fs}$ of 2.5. The WRLES prediction is in fair agreement with the measurements although some discrepancies are observed in the high frequency signal components, possibly due to the diameter size of the subminiature

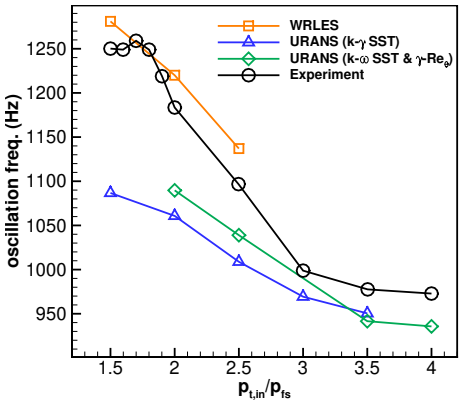

Fig. 3 Comparison of the oscillation frequencies changing with $p_{t,in}/p_{fs}$.

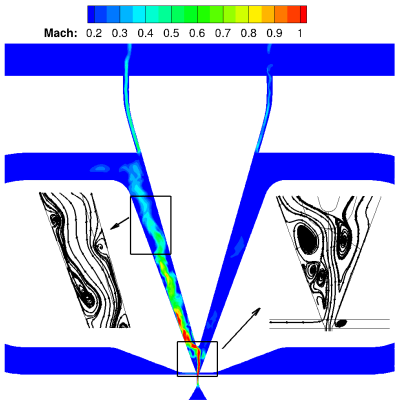

Fig. 4 Instantaneous Mach contours with streamlines during the jet switching ($p_{t,in}/p_{fs}$ = 2.0).

pressure transducer being of the same order as the loop width (see [8] for details about experimental apparatus).

Lastly, the exit velocity magnitudes are compared with the experimental data. The signal point (corresponding to the hot wire location in the experiment) is located at a distance less than a half of the outlet width from the left outlet exit, and aligned with its center (green point in Figure 1). Figure 6 displays the comparison of velocity magnitudes in a spectral domain for the $p_{t,in}/p_{fs}$ of 1.5 case. The magnitudes of the first peak which corresponds to the oscillation frequency, and of the next two peaks are in perfect agreement with the experimented ones. The differences in low and high frequency contents are caused by discrepancies due to signal durations and due to the sampling frequencies, respectively. For the rest, the spectrum, thus the pulsed jet dynamics, is well predicted by WRLES.

4 Conclusion

In this study, PJAs having different inlet pressure ratios are simulated by a high-fidelity WRLES. Oscillation frequencies as well as outlet velocities, which are the critical design parameters, are in good agreement with measurements. This study shows the importance of high-fidelity eddy resolution inside the region where recirculation and separation zones are growing during the jet switching, and where the compressible flow is highly unsteady. The next step of this study will be to analyze the time signals at different points to get further insights into the switching time as the pressure ratio changes.

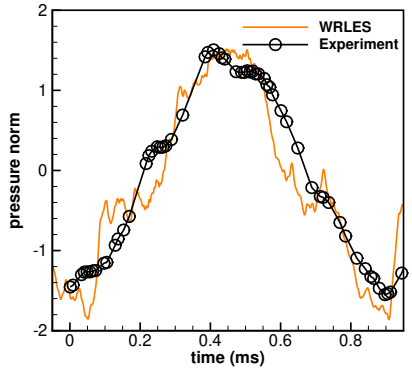

Fig. 5 Pressure norms for one oscillation period obtained from the time signals at the center of the left loop center using Z-score normalization ($p_{t,in}/p_{fs}$ = 2.5).

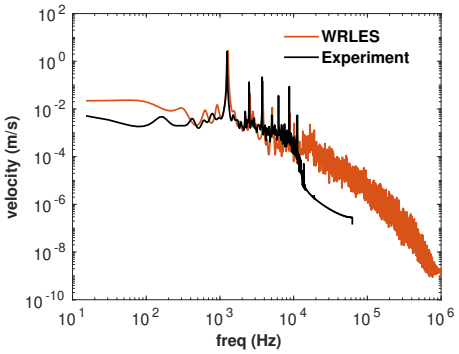

Fig. 6 Velocity magnitudes in spectral domain at the signal point close to the outlet exit ($p_{t,in}/p_{fs}$ = 1.5).

Acknowledgements This study has received funding from the Clean Sky 2 Joint Undertaking (JU) under grant agreement No 887010. The JU receives support from the European Union's Horizon 2020 research and innovation program and the CleanSky 2 JU members other than the Union. This work was granted access to the HPC resources of IDRIS and TGCC under the allocation A0092A01736 made by GENCI (Grand Equipement National de Calcul Intensif).

References

1. Aram, S. Lee, Y.T., Shan, H., Vargas, A.: Computational fluid dynamic analysis of fluidic actuator for active flow control applications. AIAA Journal. **56**(1), 111–120 (2018)
2. Cattafesta III, L.N., Sheplak, M.: Actuators for active flow control. Annual Review of Fluid Mechanics. **43**, 247–272 (2011)
3. Davidson, L.: Large eddy simulations: how to evaluate resolution. International Journal of Heat and Fluid Flow. **30**(5), 1016–1025 (2009)
4. Gloerfelt, X., Cinnella, P.: Large eddy simulation requirements for the flow over periodic hills. Flow, Turbulence and Combustion. **103**(1), 55–91 (2019)
5. Gregory, J., Tomac, M.N.: review of fluidic oscillator development and application for flow control. In: 43rd AIAA Fluid Dynamics Conference. p. 2474 (2013)
6. Kim, J., Moin, P., Seifert, A.: Large-eddy simulation-based characterization of suction and oscillatory blowing fluidic actuator. AIAA journal. **55**(8), 2566–2579 (2017)
7. Muller, H.R.: A study of the dynamic features of a wall-reattachment fluid amplifier. Journal of Basic Engineering. **86**, 819–826 (1964)
8. Saliba, G.: Study and development of fluidic micro-oscillators for cooling electronic systems. PhD thesis, Université Paul Sabatier-Toulouse III (2022)
9. Schlösser, P., Bauer, M.: Design of a pulsed jet actuator for separation control. CEAS Aeronautical Journal. **11**(4), 805–812 (2020)
10. Wang, S., Batikh, A., Baldas, L., Kourta, A., Mazellier, N., Colin, S., Orieux, S.: On the modelling of the switching mechanisms of a Coanda fluidic oscillator. Sensors and Actuators A: Physical. **299**, p. 111618 (2019)